

# Dynamic analysis and shear connector damage identification of steel-concrete composite beams

Zhongming Hou<sup>1</sup>, He Xia\*<sup>1</sup> and YanLing Zhang<sup>2</sup>

<sup>1</sup>School of Civil Engineering, Beijing Jiaotong University, Beijing, 100044, China

<sup>2</sup>School of Civil Engineering, Shijiazhuang Tiedao University, Shijiazhuang, 050043, China

(Received February 01, 2012, Revised April 26, 2012, Accepted June 24, 2012)

**Abstract.** With the advantages of large span, light deadweight and convenient construction, the steel-concrete composite beam (SCCB) has been rapidly developed as a medium span bridge. Compared with common beams, the global stiffness of SCCB is discontinuous and in a staged distribution. In this paper, the analysis model for the simply-supported SCCB is established and the vibration equations are derived. The natural vibration characteristics of a simply-supported SCCB are analyzed, and are compared with the theoretical and experimental results. A curvature mode measurement method is proposed to identify the shear connector damage of SCCB, with the stiffness reduction factor to describe the variation of shear connection stiffness. By analysis on the 1<sup>st</sup> to 3<sup>rd</sup> vertical modes, the distribution of shear connectors between the steel girder and the concrete slab are well identified, and the damage locations and failure degrees are detected. The results show that the curvature modes can be used for identification of the damage location.

**Keywords:** steel-concrete composite beam; shear connector; dynamic behavior; curvature mode; damage identification; stiffness reduction factor.

---

## 1. Introduction

With the advantages of large span, light deadweight and convenient construction, the steel-concrete composite beam (SCCB) has been rapidly developed as a medium span bridge. However, due to the structural characteristics of SCCB, fatigue damage is easy to appear in the shear connectors, and the adjacent steel girder and concrete slab, but it is difficult to detect the damage due to the sheltered position of shear connectors.

Numerous researches on bridge damage identification have been carried out, and many identification methods proposed, by which the potential damage of structures were deduced from the static or dynamic variation behaviors, such as damage finding, damage location and damage degree determination. However, these researches were mainly focused on common bridges (Ansourian 1981, Dilena *et al.* 2011) or buildings (Ryu *et al.* 2004, Chen *et al.* 2011).

For composite beam bridges, Huang and Su (2005) derived the governing equations of motion for partial composite beams based on the one-dimensional partial composite beam theory; Xu and Wu (2007) investigated the static, dynamic and buckling behaviors of partial interaction composite members

---

\* Corresponding author, Professor, E-mail: [hxia88@163.com](mailto:hxia88@163.com)

by taking into account the influences of rotary inertia and shear deformations. Girhammar *et al.* (2009) derived the partial differential equations for the composite Euler-Bernoulli members with interlayer slip subjected to general dynamic loading, and presented general solutions for the deflection, internal action and related boundary conditions. Some experimental researches (Morassi and Rocchetto 2003, Dilena and Morassi 2003, Liu *et al.* 2009a) and numerical analyses (Jiang *et al.* 2006, Liu *et al.* 2008, 2009b) on railway steel-concrete composite beam bridges were conducted, and the results for their natural vibration characteristics and dynamic responses were presented. Ye and Huang (2005) conducted damage identification for a steel-concrete composite beam model of a high-speed railway bridge by simulating various damage cases, in which natural frequencies, mode shapes and curvature modes were adopted as the identification indicies. By analyzing its undamped free vibration, they studied the relationship between the damage index and the structure damage, and then simulated the damage of various degrees by reducing the bending stiffness in different position of the beam. Xia *et al.* (2007) constructed a 1:3 scaled bridge model to test the suitability and efficiency of various vibration-based damage identification methods, and assessed the integrity of the shear connectors. Up to now, however, very few damage identification methods specified for shear connectors of SCCB were discussed.

The current paper is mainly concerned with the dynamic characteristics and shear connector damage identification method of SCCB. The analysis model for the simply-supported SCCB is established and the vibration equations are derived; The natural vibration characteristics of a simply-supported test SCCB are analyzed using FEM software, and are compared with the theoretical and experimental results. A curvature mode measurement method is proposed to identify the shear connector damage of SCCB, with the stiffness reduction factor to describe the variation of shear connection stiffness.

## 2. Basic analysis model

SCCB is composed of concrete slab and steel girder. To establish the dynamic analysis model for SCCB, the following basic assumptions are adopted:

- (1) The concrete slab and the steel girder accord with the plane surface assumption.
- (2) There is no lift displacement between the concrete slab and the steel girder.
- (3) The shear force borne by shear connectors is uniformly distributed along the interface.
- (4) Only small deformation occurs in the structure.

According to the structural characteristic of SCCB, the analysis model is divided into two sub-beams: the concrete slab and the steel girder. A micro-element model for the SCCB with unit longitudinal shear stiffness  $K_S$  is shown in Fig. 1.

Suppose the shear force borne by shear connectors can be expressed as  $Q_L(x) = K_S \delta dx$ , the following relationship is obtained

$$\delta = (\theta + \nu')h \quad (1)$$

where  $\delta$  is the relative slip between the concrete slab and the steel girder, which causes a rotation angle  $\theta$  of their gravity connecting line from the vertical direction;  $\nu'$  is the corresponding rotation angle of the slab and the girder.

By the direct equilibrium method, the equation of motion can be obtained as

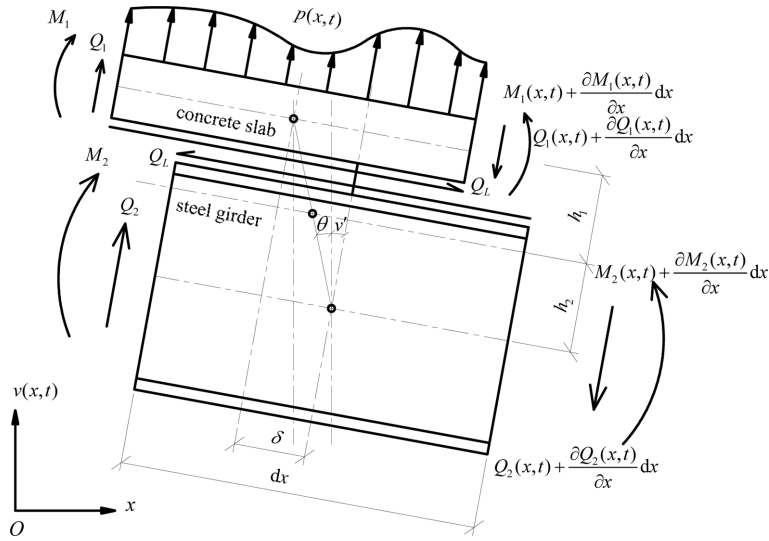


Fig. 1 Analysis model of micro-element for SCCB

$$(EI)_B \frac{\partial^4 v(x,t)}{\partial x^4} + m(x) \frac{\partial^2 v(x,t)}{\partial t^2} + c(x) \frac{\partial v(x,t)}{\partial t} = p(x,t) + K_S h^2 (\theta' + v'') \quad (2)$$

where:  $(EI)_B = E_1 I_1 + E_2 I_2$ , is the bending stiffness of the concrete slab and steel girder that around the centroid axis of themselves;  $E$  is modulus of elasticity;  $I$  is moment of inertia; the subscripts 1 and 2 represent the concrete slab and the steel girder, respectively;  $v(x, t)$ ,  $m(x)$  and  $c(x)$  are, respectively, the vertical displacement, unit mass and damping coefficient of the beam; and  $p(x, t)$  is the dynamic load.

For a micro-element of  $dx$ , we have the following relationship

$$K_S h^2 (\theta + v') = (EI)_C \theta'' \quad (3)$$

where,  $(EI)_C = E_1 A_1 h_1^2 + E_2 A_2 h_2^2$ , is the bending stiffness of the concrete slab and steel girder that around the centroid axis of the whole beam;  $A_1$  and  $A_2$  are the areas of the concrete slab and steel girder,  $h_1$  and  $h_2$  are the distances from the centroid axes of themselves to the neutral axis of the beam.

If  $m(x)$  and  $c(x)$  are considered as constants, and respectively expressed as  $\bar{m}$  and  $\bar{c}$ , and utilizing Eq. (3), the equation of motion Eq. (2) becomes

$$\begin{aligned} \frac{\partial^6 v(x,t)}{\partial x^6} - \frac{K_S h^2 (EI)_F}{(EI)_C (EI)_B} \frac{\partial^4 v(x,t)}{\partial x^4} + \frac{\bar{m}}{(EI)_B} \frac{\partial^4 v(x,t)}{\partial x^2 \partial t^2} + \frac{\bar{c}}{(EI)_B} \frac{\partial^2 v(x,t)}{\partial x \partial t} - \frac{K_S h^2 \bar{m}}{(EI)_C (EI)_B} \frac{\partial^2 v(x,t)}{\partial t^2} \\ = \frac{1}{(EI)_B} \frac{\partial^2 p(x,t)}{\partial x^2} - \frac{K_S h^2 p(x,t)}{(EI)_C (EI)_B} \end{aligned} \quad (4)$$

where:  $(EI)_F = (EI)_C + (EI)_B$  is the equivalent stiffness of the beam, which is the section stiffness identical with that concrete slab and steel girder are fully glued.

Assume the solution has a form  $v(x, t) = \phi(x) \cdot q(t)$ , the motion equation after variable separation can be expressed as

$$\frac{d^6 \phi(x)}{dx^6} - \frac{K_S h^2 (EI)_F}{(EI)_C (EI)_B} \frac{d^4 \phi(x)}{dx^4} - \frac{\bar{m} \omega^2}{(EI)_B} \frac{d^2 \phi(x)}{dx^2} + \frac{K_S h^2 \bar{m} \omega^2 \phi(x)}{(EI)_C (EI)_B} = 0 \quad (5)$$

in which  $\phi(x)$  represents the mode shape and  $q(t)$  the modal amplitude. The mode shape can be expressed as

$$\phi(x) = A \sinh \lambda_1 x + B \cosh \lambda_1 x + C \sinh \lambda_2 x + D \cosh \lambda_2 x + E \sin \lambda_3 x + F \cos \lambda_3 x \quad (6)$$

where  $A, B, C, \dots$  are constants determined by the boundary conditions. For a straight simply-supported beam, the boundary conditions can be expressed as

$$\begin{aligned} \phi(0) &= 0 & \phi(L) &= 0 & \phi''(0) &= 0 \\ \phi''(L) &= 0 & \phi''''(0) &= 0 & \phi''''(L) &= 0 \end{aligned} \quad (7)$$

Substituting them into Eq. (6), a sextic homogeneous equation set is obtained, in which the determinant of the coefficient matrix must be equal to zero to get a set of nonzero solution for the coefficients in Eq. (6). Finally, the determinant can be given as

$$(\lambda_2^2 - \lambda_1^2)^2 (\lambda_1^2 + \lambda_3^2)^2 (\lambda_3^2 + \lambda_2^2)^2 \sinh \lambda_1 L \sinh \lambda_2 L \sin \lambda_3 L = 0 \quad (8)$$

Thus  $\phi_n(x) = \sin \lambda_3 x = \sin(n\pi x/L)$ . The circular frequencies can be solved by substituting  $\lambda = \pm i\lambda_3 = \pm i n\pi/L$  into Eq. (5) as

$$\omega_n^2 = \frac{(n\pi)^4 (EI)_F}{\bar{m} L^4} \frac{1 + \beta + (n\pi)^2 \alpha}{(1 + \beta)[1 + (n\pi)^2 \alpha]} \quad (9)$$

where  $\alpha = (EI)_C / (K_S h^2 L^2)$ , and  $\beta = (EI)_C / (EI)_B$ . For an SCCB with a uniform cross section, factor  $\beta$  is a constant, while factor  $\alpha$  varies with the shear connection degree.

The factor  $\alpha$  in Eq. (9) reflects the connection degree of the steel girder and concrete: the smaller  $\alpha$  is, the greater the shear stiffness of the connectors become, and the same as the shear connection degree; when  $\alpha$  approaches to zero, the shear stiffness  $K_S$  of connectors will approach to infinite, in this case, we have

$$\omega_{n,F} = \frac{(n\pi)^2}{L^2} \sqrt{\frac{(EI)_F}{\bar{m}}} \quad (10)$$

which is the same as a common straight beam. For the straight SCCB

$$\omega_n^2 = \frac{1 + \beta + (n\pi)^2 \alpha}{(1 + \beta)[\alpha(n\pi)^2 + 1]} \omega_{n,F}^2 = \gamma^2 \omega_{n,F}^2 \quad (11)$$

where  $\gamma^2 = \frac{1 + \beta + (n\pi)^2 \alpha}{(1 + \beta)[\alpha(n\pi)^2 + 1]}$ .

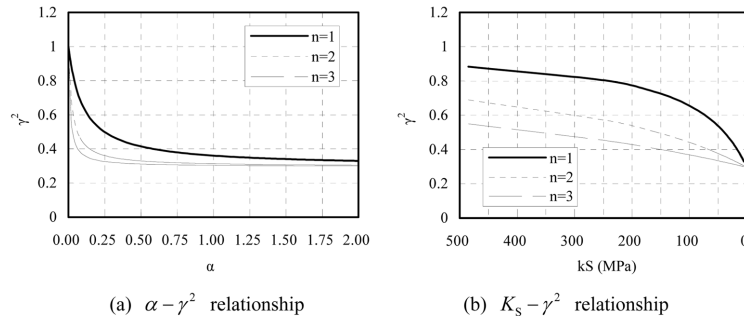


Fig. 2 Relationships of  $\alpha - \gamma^2$  and  $K_S - \gamma^2$

It can be known from Eq. (11) that factor  $\gamma^2$  directly reflects the influence of the shear connection degree. For the vertical natural frequency, let  $\beta = 0.234$ , which is concerned with the simply-supported SCCB in Section 3, the relationships between factors  $\alpha$  and  $\gamma^2$ ,  $K_S$  and  $\gamma^2$  ( $n = 1, 2, 3$ ) are obtained, as shown in Fig. 2.

Figs. 2(a) and 2(b) are the expressions of  $\gamma^2$  with different variables. It can be seen from Fig. 2(a) that when  $\alpha$  tends to zero, i.e.,  $K_S$  tends to infinite, the beam is equivalent to an integral one without interface slip between the slab and the girder, and all orders of  $\gamma^2$  approaches to 1. When  $\alpha$  tends to infinite, i.e.,  $K_S$  tends to zero, the beam is equivalent to a separate one without shear connector, and all orders of  $\gamma^2$  tends to become a constant, which is about 0.296 in the figure. In addition, one can see the increase of  $n$  leads to a sharper descending of  $\gamma^2$ . In the common layout of shear connectors, the equivalent stiffness of SCCB expressed as  $\gamma^2(EI)_F$  decreases with the degradation of shear connection stiffness, which shows a decreasing tendency of  $\gamma^2$  in Fig. 2, and corresponding frequency reduction of the vertical natural frequency; When the shear connection stiffness reduces to a certain extent,  $\gamma^2$  tends to become a constant (Fig. 2(b)).

From the above analysis, it can be known that for the SCCB composed of two different materials, its dynamic characteristics are different from that of the common beam with homogenous material. The connection degree between steel girder and concrete slab directly influences the dynamic characteristics of the composite beam. The factor  $\gamma^2$  varies with shear connection stiffness, which is herein defined as “stiffness reduction factor” for the vertical dynamic response of SCCB.

### 3. Verification of numerical analysis results

A dynamic experiment on six test SCCBs with different connection stiffnesses was conducted, from which the natural vibration characteristics of the beams were obtained, and are used to verify the theoretical and numerical results.

#### 3.1 Parameters of the test beam

The test beams, with a span of 4200 mm and a box section, is composed of Q235 steel girder and C30 concrete deck. The steel girder is 200 mm high, with its bottom flange 400 mm wide and 8 mm thick, and its web 6 mm thick. The concrete deck is 700 mm wide for PCB and 70 mm thick. The connector diameter is 13 mm, with the height of 50 mm, and space of 210 mm. There are two types in the six

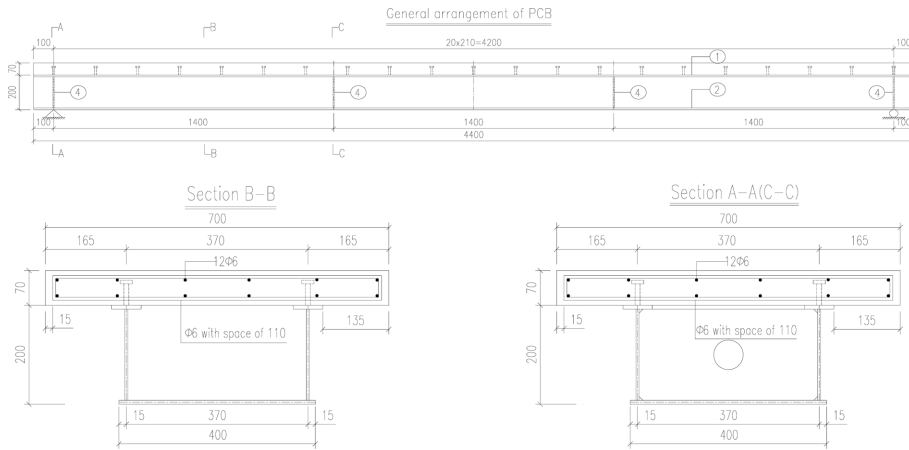


Fig. 3 Dimensions of the test beam (unit: mm)

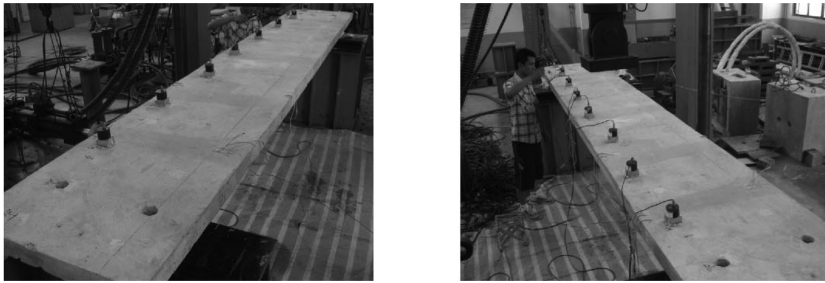


Fig. 4 The beam under test

beams: full connection and partial connection. A beam that is with partial connection (PCB) is selected as the research object, as shown in Figs. 3 and 4 is the photo of the beam under test.

### 3.2 Dynamic characteristics of SCCB model

Based on the FE software ANSYS, a finite element model is established for the test beam, as shown in Fig. 5. The concrete slab and the steel girder shell are modeled, respectively, with elements SHELL91 and SHELL43, and the slip between the steel girder and concrete slab is considered. The three-directional spring element COMBIN39 is set at the position of each connector; the nodes between the concrete slab and steel girder are coupled in the vertical and transverse direction, but not in the longitudinal directions. For the simply-supported SCCB, constraints of  $U_x$ ,  $U_y$ ,  $R_x$  are applied to nodes at one support, and  $U_y$ ,  $R_x$  at another. The shear-slip curve of shear connector can be defined by  $Q = Q_u(1 - e^{-\beta s})^\alpha$ , where  $Q_u = 46382$  N is the ultimate load of the connector according to the test result, and the coefficients  $\alpha = 0.70$ ,  $\beta = 0.80$  are determined from the experimental results (Zhang 2009, Gattesco 1999, also see Eurocode 4 1994).

Applying the above parameters to the finite element model, the natural frequencies and mode shapes are calculated. The first nine orders of modes are described in Fig. 6.

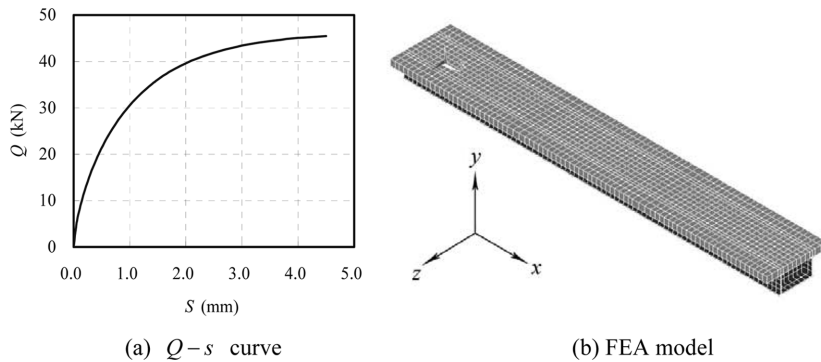


Fig. 5 The constitutive relationship of  $Q-s$  and the FE model of the SCCB

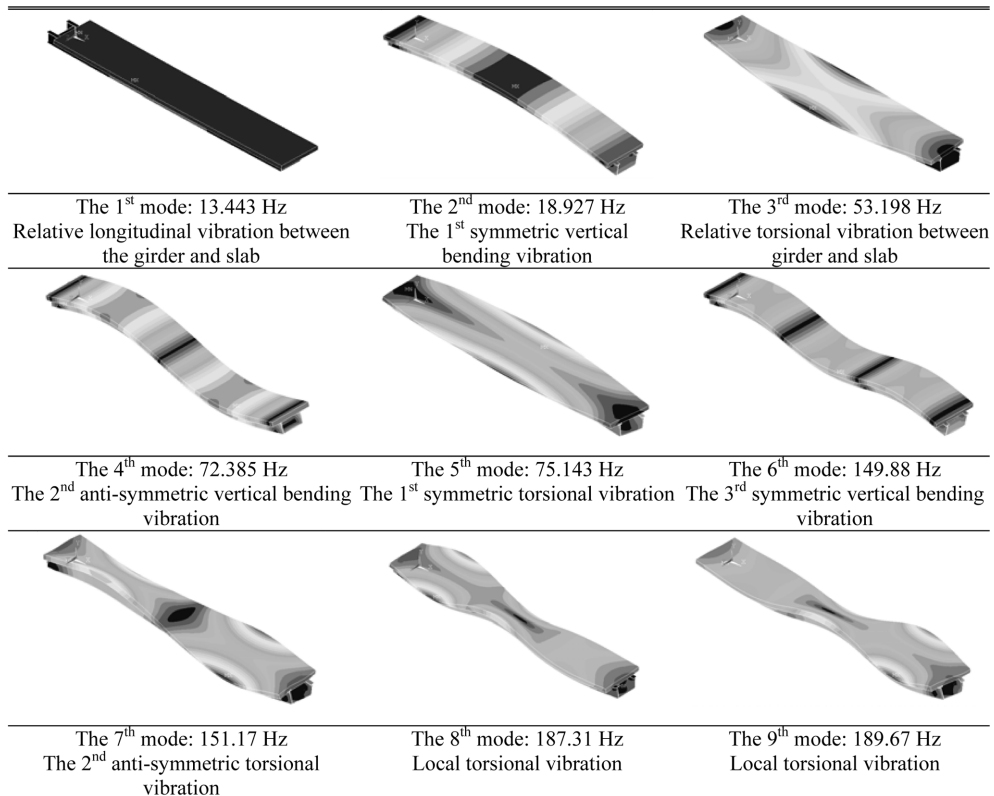


Fig. 6 The first nine natural frequencies and mode shapes of SCCB with partial connection

From Fig. 6 one can see that the vertical modes keep consistent between the concrete slab and steel girder, but there is obvious phase difference between the longitudinal modes. Due to the shear deformation of flexible connectors, relative slip occurs at the interface of the composite beam, which makes the mode shapes of the concrete slab and steel girder neither isochronous nor harmonious.

Obviously, the relative slip between the concrete slab and steel girder has a notable influence on the dynamic behaviors of SCCB, which makes the global stiffness of the beam decreased, and consequently

Table 1 Comparisons among the theoretical, numerical and experimental results (vertical bending vibration)

No.	Mode order	Theoretical result (Hz)	Numerical result (Hz)	Experimental result (Hz)
1	The 1 <sup>st</sup>	21.74	18.927	18.875
2	The 2 <sup>nd</sup>	71.52	72.385	88.750
3	The 3 <sup>rd</sup>	148.72	149.88	144.011

a falling in the frequency. The first vertical frequency is 28.91 Hz when the slip effect is ignored, while 18.927 Hz when the slip effect is considered according to the shear connector layout assumption. Referring to the above calculating result, the stiffness reduction factor  $\gamma^2$  is calculated as 0.429. The comparisons among the theoretical, numerical and experimental results are shown in Table 1.

It can be seen that the numerical and experimental results of the first vertical frequency are close, but both of them are smaller than the theoretical results. As for the second and the third vertical frequencies, all the results accord well except for the experimental result of the second order, where there is a certain deviation. The deviation appeared to have been mainly caused by many factors; one possible reason is the boundary condition, which has considerable influence upon the test result. Certainly, the bond force at the interface of the beam and the measurement error also has a certain impact, but plays a minor role. In general, the theoretical, numerical and experimental values accord well, thus the finite element model is validated.

It can be concluded that the SCCB has different dynamic characteristics compared with common beams, where the feature of shear connectors plays an important role. Under the flow of traffic cyclic loads, the shear connectors of the SCCB are easily subjected to fatigue damage due to repeated shear force, so it is necessary to seek out an effective method to identify the damage.

#### 4. Damage identification method and numerical analysis for SCCB

For a civil engineering structure, normally, local damage will not cause obvious change in its natural frequencies or mode shapes. Therefore, it is important to select a highly-sensitive damage identification index that suits the structure. There have been various damage identification indices based on mode shapes, such as COMAC (Coordinate Assurance Modal Criteria) (e.g., Brasiliano 2004), curvature mode difference, modal element energy, modal flexibility matrix (e.g., Votsis 2009, Reynders 2010), and there are damage identification methods based on strain modal, such as strain modal difference (e.g., Unger *et al.* 2005, Asgarian *et al.* 2009). Also, some identification methods, such as wavelet transform (e.g., Gokdag 2011, Montejo Luis 2011), multi-source information fusion (MSIF) (e.g., Liu *et al.* 2009), are gradually applied. Furthermore, some sensitivity analyses of mechanical behaviors for bridge damage assessment are proposed (e.g., Miyamoto and Isoda 2012). Considering the connection between steel girder and concrete slab, i.e., the global stiffness of steel-concrete composite beam, is discontinuous and in a staged distribution, then curvature mode method, which is sensitive to the stiffness, is adopted for the damage identification of SCCB.

##### 4.1 Damage identification method

According to material mechanics and structural dynamics, the curvature variation function of the beam in flexural vibration is given as

$$\frac{M}{EI(x)} = k(x, t) = \frac{1}{\rho(x, t)} = \frac{\partial^2 u(x, t)}{\partial x^2} = \sum_{n=1}^{\infty} \phi_n''(x) q_n(t) \quad (12)$$

where,  $M$ ,  $E$  and  $I(x)$  are the moment, modulus of elasticity and moment of inertia, respectively;  $k(x, t)$ ,  $\rho(x, t)$  and  $\phi_n''(x)$  are the curvature, the radius of curvature and the  $n^{\text{th}}$  curvature mode of the beam respectively.

This function indicates a direct correspondence between the curvature  $u''(x, t)$  and the curvature mode  $\phi_n''(x)$ . From Eq. (12) one can know that the curvature mode changes with the beam's stiffness, namely, it is sensitive to the structure damage, and corresponds to the displacement.

Although the curvature mode shapes of the structure are very difficult to measure, they can be approximately calculated with the central difference method. For the  $n^{\text{th}}$  mode, the curvature mode at the  $i^{\text{th}}$  node can be expressed as

$$\phi_{ni}''(x) = \frac{\phi_n(i+1) - 2\phi_{ni} + \phi_n(i-1)}{l^2} \quad (13)$$

where,  $l$  is the distance between two adjacent measuring points.

To decrease the calculating error, this method requires enough placement density of measuring point or very good precision of interpolation of extended order modes.

From Eq. (11) one can see, the global stiffness of the simply-supported SCCB can be expressed as

$$(EI)_{eq} = \frac{1 + \beta + (n\pi)^2 \alpha}{(1 + \beta)[1 + (n\pi)^2 \alpha]} (EI)_F \quad (14)$$

Considering two extreme connection cases between the steel girder and concrete slab: one is fully-separated, just a simple cascade, where the shear stiffness of the shear connector  $K_S$  is zero; the other is completely-glued, where  $K_S$  equals to infinity. The equivalent stiffness for the two extreme cases are  $(EI)_{eq1} = (EI)_B$  and  $(EI)_{eq2} = (EI)_C + (EI)_B = (EI)_F$ , respectively, and the real connecting stiffness is between  $(EI)_{eq1}$  and  $(EI)_{eq2}$ . The connecting degree between steel girder and concrete slab can be described by factors  $\alpha$  and  $\beta$ , as mentioned in Section 2.

In practical layout of shear connectors, the connection between steel girder and concrete slab is discontinuous, and they are connected by shear connectors installed with a distance. The stiffness of the SCCB in Eq. (14) is actually an average value in a certain area, which is a macroscopical parameter. Seen from the local structure near the shear connectors, the beam's stiffness shows the characteristic of an integrated beam, while between the shear connector rows, it shows the characteristic of a "laminated beam".

The stiffness of SCCB presents a staged distribution. Owing to the distribution of shear connectors, SCCB has a relative large stiffness near the connecting points, and the corresponding curvature curve shows an obvious discontinuity. Under static or dynamic load, therefore, a series of peaks appear at the location of the shear connectors.

In other words, when damage occurs at shear connectors, the local stiffness and the corresponding curvature mode curve will change. Based on the above principle, the curvature mode method is used to identify the damage in shear connectors. Considering the connectors' characteristics, the forward or the backward difference method is applied to calculate the curvature mode of the SCCB, that is

$$\phi_{ni}'(x) = \frac{\phi_n(i) - \phi_n(i-1)}{\Delta l}, \quad \phi_{ni}''(x) = \frac{\phi_n'(i) - \phi_n'(i-1)}{\Delta l^2} \quad (15)$$

#### 4.2 Numerical analysis

There are eight models for the SCCB with different connection conditions, as shown in Table 2. The damage of shear connectors is simulated by removing the related connector elements. In the analysis, only the longitudinal slip between steel girder and concrete slab is considered, therefore only the vertical modes for the eight models are extracted.

In the table, PCB means “damage of the partial connection composite beams”, the following numbers stand for the damage location of the shear connectors. A shear connector row may contain one or more connectors along the cross direction, as shown in Fig. 7.

##### (1) Natural frequencies extracted from FEA results

Listed in Table 3 are the analyzed frequencies of the models, in which the bold, boxed and underlined values represent the first, second and third vertical natural frequencies, respectively.

Largely, one can find that the natural frequencies of the 1<sup>st</sup>, 2<sup>nd</sup> and 3<sup>rd</sup> vertical mode show a decreasing tendency versus the location of damage from the boundary to the midspan of the beam, and

Table 2 Operation conditions under different degrees of damage

No.	Model	Damage location	Note
1	PCB-1&2	At the 1 <sup>st</sup> and 2 <sup>nd</sup> connector rows	Remove the connector
2	PCB-1&3	At the 1 <sup>st</sup> and 3 <sup>rd</sup> connector rows	Remove the connector
3	PCB-1	At the 1 <sup>st</sup> connector rows	Remove the connector
4	PCB-2	At the 2 <sup>nd</sup> connector rows	Remove the connector
5	PCB-3	At the 3 <sup>rd</sup> connector rows	Remove the connector
6	PCB-4	At the 4 <sup>th</sup> connector rows	Remove the connector
7	PCB-5	At the 5 <sup>th</sup> connector rows	Remove the connector
9	PCB-0	No damage of the connector rows	/

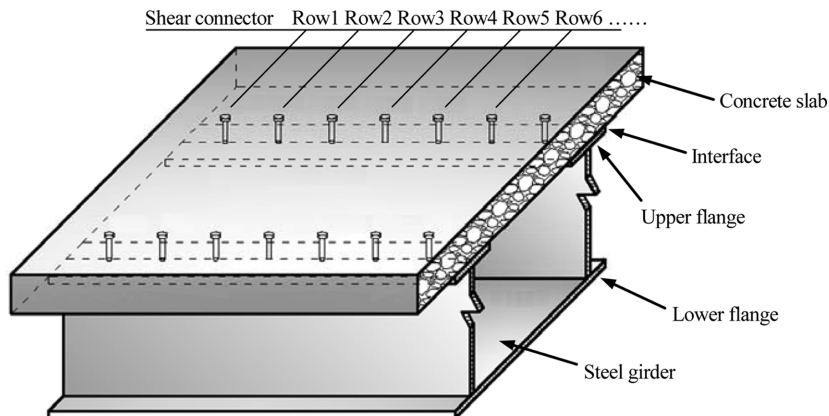


Fig. 7 Shear connector arrangement of the SCCB

Table 3 Natural frequencies of eight models with different degrees of damage

Mode	PCB-1&2	PCB-1&3	PCB-1	PCB-2	PCB-3	PCB-4	PCB-5	PCB-0
1	12.799	12.800	13.127	13.127	13.126	13.126	13.126	13.443
2	18.890	18.899	18.911	18.913	18.913	18.914	18.915	18.927
3	29.992	38.769	40.169	53.163	53.192	53.194	53.195	53.198
4	66.748	70.509	70.843	72.369	72.366	72.355	72.346	72.385
5	71.823	72.341	72.352	75.078	75.125	75.141	75.141	75.143
6	81.542	86.802	88.797	149.78	149.68	149.58	149.61	149.88
7	92.710	149.60	149.68	151.02	151.13	151.13	151.12	151.17
8	137.14	154.20	154.33	187.18	187.14	187.08	187.07	187.31
9	150.72	184.94	184.97	189.54	189.63	189.65	189.65	189.67

the damage near the boundary (e.g., PCB-1, PCB-2) shows more obvious effect on the frequency. Compared with the model without damage (PCB-0), it can be known that the damage of the shear connectors decreases the vertical frequencies of the beam. However, although the damage occurrence can be preliminarily identified from the decrease of natural frequencies, the damage location and degree are still unknown.

(2) Mode shapes of all models extracted from FEA results

Shown in Fig. 8 are the first, second and third vertical mode shapes for the eight models, in which the abscissa axis represents the location from the left bearing.

It can be seen that there is no obvious difference among the first mode shapes of the eight models. For the second and the third mode, the mode shapes show obvious discrepancy only under a relatively

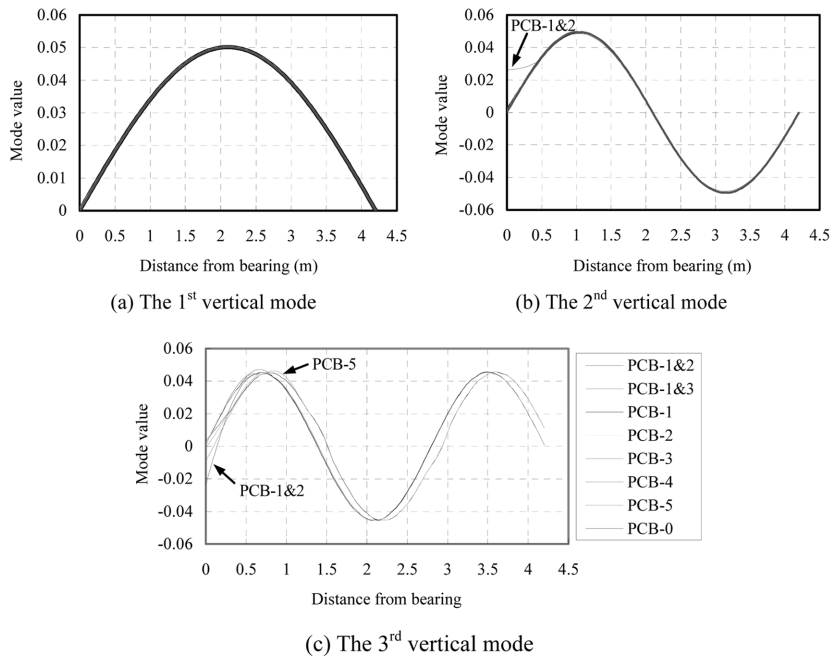


Fig. 8 Vertical mode shapes of partial connection composite beam before and after damage

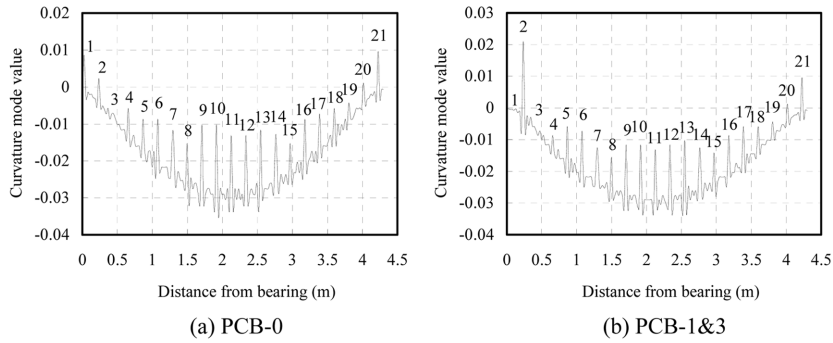


Fig. 9 The 1<sup>st</sup> vertical curvature modes of the beams without and with damage

serious damage (for instance, PCB-1&2). Likewise, although the damage occurrence can be preliminarily identified from the changing of mode shapes, among which there are still no striking contrast.

(3) Curvature modes extracted from the first mode shapes

From the above curves, however, it is still difficult to identify the damage scope and degree of shear connectors. Therefore, a forward difference with the above mode shape data is conducted. Taking the cases PCB-0 and PCB-1&3 for instance, the curvature modes of the composite beam are shown in Fig. 9.

There are 19 shear connector rows in PCB-0 and PCB-1&3. When the first and third shear connector rows of PCB-1&3 are removed, the damage position is very clear. While for PCB-0, although no

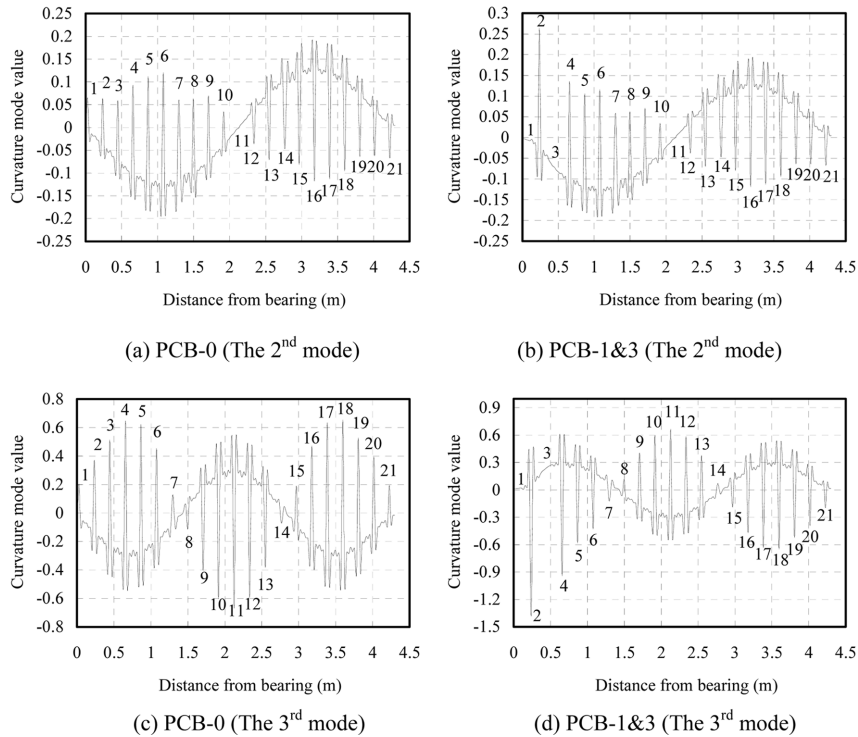


Fig. 10 The 2<sup>nd</sup> and 3<sup>rd</sup> vertical curvature modes of the beams without and with damage

damage there, the first and the third peaks in its first vertical curvature mode disappear. The damage is apt to be misjudged in such case.

Due to the discontinuity of stiffness, if some shear connectors are removed in certain location, the stiffness and the mechanical characteristic there are similar to that no shear connectors are placed, and the corresponding curvature mode peak will decrease or even disappear eventually. It is noteworthy that curvature mode curve will show a sharp change in the position of adjacent shear connectors, as shown in Fig. 9(b). When serious damage occurs, the stiffness of the beam in this location will show a certain characteristic like that between two shear connector rows, thereafter peaks in the corresponding curvature mode will disappear, thus the damage degree and location can be shown consequently.

#### (4) Curvature modes extracted from the second and third mode shapes

A further observation on the second and the third vertical curvature curves is performed, as shown in Fig. 10.

Figs. 9 and 10 indicate that when damage occurs in certain position, the corresponding curves will show an obvious variation, and all peaks in the 1<sup>st</sup> to 3<sup>rd</sup> (or even more) curvature modes there will change. In this instance, there are 21 shear connector rows between the steel girder and concrete slab, which shows 21 peaks. For PCB-1&3, only 19 shear connector rows are successfully identified when damage occurs at the first and the third connector rows. Therefore, damage identification of the the first and the third connector rows is achieved (as marked in Fig. 10 with red arrows)

This case study shows that the damage position and scope of the composite beam are effectively identified with the curvature modes. If more curvature modes are comprehensively considered, the identification results are more accurate. By the same way, the longitudinal and lateral curvatures can also be used to identify damage of shear connectors.

It should be pointed out that in practical mode measurements, a relatively large error will occur if the measuring points are not sufficient in the damage position, or the excitation force is not big enough. Likewise, the support conditions as well as the distribution density of measuring points are also crucial to the identification results.

## 5. Conclusions

Starting from derivation of the governing motion equations for the composite beam, the dynamic characteristics and “stiffness reduction factor” have been developed and applied to a test SCCB by carrying out FE analysis and dynamic experiment. A curvature mode measurement method is proposed to identify the shear connector damage of SCCB. Some conclusions are obtained as follows

(1) The dynamic characteristics of SCCB are different from those of the common beam with homogenous material. The slip at the interface will directly influence the integral stiffness, the vertical natural frequencies and mode shapes of SCCB.

(2) The vertical modes of SCCB can keep consistent between the concrete slab and the steel girder, but there is a phase difference between their longitudinal modes due to the deformation of shear connectors, which makes their mode shapes neither isochronous nor harmonious.

(3) Compared with common beams, the global stiffness of steel-concrete composite beam is discontinuous and in a staged distribution.

(4) The distribution, position and scope of the shear connector damage can be identified effectively by the curvature mode measurement method, and a further forward difference to curvature mode will offer better identification effect.

## Acknowledgements

The research is supported by the State Fundamental Research Funds “973” Program (2013CB036203) and the Natural Science Foundation of China (No. 51078029, 51108281).

## References

- Ansourian, P. (1981), “Experiments on continuous composite beams”, *Proc. Instn. Civ. Eng.*, Part 2, **71**(12), 25-71.
- Asgarian, B., Amiri, M. and Ghafooripour, A. (2009), “Damage detection in jacket type offshore platforms using modal strain energy”, *Struct. Eng. Mech.*, **33**(3), 325-337.
- Brasiliano, A., Doz, G.N. and de Brito, J.L.V. (2004), “Damage identification in continuous beams and frame structure using the Residual Error Method in the Movement Equation”, *Nucl. Eng. Des.*, **227**(1), 1-17.
- Chen, W.H., Lua, Z.R. and Lin, W., *et al.* (2011), “Theoretical and experimental modal analysis of the Guangzhou New TV Tower”, *Eng. Struct.*, **33**(12), 3628-3646.
- Dilena, M., Morassi, A. and Perin, M. (2011), “Dynamic identification of a reinforced concrete damaged bridge”, *Mech. Syst. Signal. Pr.*, **25**(8), 2990-3009.
- Dilena, M. and Morassi, A. (2003), “A Damage Analysis of Steel-Concrete Composite Beams Via Dynamic Methods: Part II. Analytical Models and Damage detection”, *J. Vib. Control*, **9**(5), 529-565.
- Eurocode 4, European Standard. (2007), *Design of composite steel and concrete structures*, Part 1.1: General rules and rules for buildings-General rules, EN 1994-1-1.
- Gattesco, N. (1999), “Analytical modeling of nonlinear behavior of composite beams with deformable connection”, *J. Constr. Steel Res.*, **52**(2), 195-218.
- Girhammar, U.A., Pan, D.H. and Gustafsson, A. (2009), “Exact dynamic analysis of composite beams with partial interaction”, *Int. J. Mech. Sci.*, **51**(8), 565-582.
- Gokdag, H. (2011), “Wavelet-based damage detection method for a beam-type structure carrying moving mass”, *Struct. Eng. Mech.*, **38**(1), 81-97.
- Huang, C.W. and Su, Y.H. (2008), “Dynamic characteristics of partial composite beams”, *Int. J. Struct. Stab. D.*, **8**(4), 665-685.
- Jiang, L.Z., Ding, F.X. and Yu, Z.W. (2006), “Experimental study on the integrated dynamic behavior of continuous steel-concrete composite girders of railway bridges”, *China Railway Science*, **27**(5), 60-65, (*in Chinese*).
- Liu, K. and De Roeck, G. (2008), “Damage detection of shear connectors in composite bridges”, *Proceedings of Isma 2008: International Conference on Noise and Vibration Engineering*, Leuven, Belgium, September.
- Liu, K., De Roeck, G. and Lombaert, G. (2009a), “The effect of dynamic train-bridge interaction on the bridge response during a train passage”, *J. Sound. Vib.*, **325**(1-2), 240-251.
- Liu, K., Reynders, E., De Roeck, G. and Lombaert, G. (2009b), “Experimental and numerical analysis of a composite bridge for high-speed trains”, *J. Sound. Vib.*, **320**(1-2), 201-220.
- Liu, T., Li, A.Q., Ding, Y.L. and Zhao, D.L. (2009), “Study of the structural damage identification method based on multi-mode information fusion”, *Struct. Eng. Mech.*, **31**(3), 333-347.
- Miyamoto, A. and Isoda, S., (2012), “Sensitivity analysis of mechanical behaviors for bridge damage assessment”, *Struct. Eng. Mech.*, **41**(4), 539-558.
- Montejo Luis, A. (2011), “Signal processing based damage detection in structures subjected to random excitations”, *Struct. Eng. Mech.*, **40**(6), 745-762.
- Morassi, A. and Rocchetto, L. (2003), “A Damage Analysis of Steel-Concrete Composite Beams Via Dynamic Methods: Part I. Experimental Results”, *J. Vib. Control*, **9**(5), 507-527.
- Reynders, E. and De Roeck, G. (2010), “A local exibility method for vibration-based damage localization and quantification”, *J. Sound. Vib.*, **329**(12), 2367-2383.
- Ryu, H.K., Shim, C.S., Chang, S.P. and Chung, C.H. (2004), “Inelastic behaviour of externally prestressed continuous composite box-girder bridge with prefabricated slabs”, *J. Constr. Steel Res.*, **60**(7), 989-1005.
- Unger, J.F., Teughels, A. and De Roeck, G. (2005), “Damage Detection of a Prestressed Concrete Beam Using

- Modal Strains”, *J. Struct. Eng. -ASCE.*, **131**(9), 1456-1463.
- Votsis Renos, A. and Chryssanthopoulos Marios, K. (2009), “Assessment of debonding in GFRP joints using damage identification techniques”, *Constr. Build. Mater.*, **23**(4), 1690-1697.
- Xia, Y., Hao, H. and Deeks, A.J. (2007), “Dynamic assessment of shear connectors in slab-girder bridges”, *Eng. Struct.*, **29**(7) 1475-1486.
- Xu, R.Q. and Wu, Y.F. (2007), “Static, dynamic, and buckling analysis of partial interaction composite members using Timoshenko’s beam theory”, *Int. J. Mech. Sci.*, **49**(10) 1139-1155.
- Ye, M.X. and Huang, Q. (2005), “Damage detection of high-speed railway steel concrete composite beam”, *J. Cent. South. Univ. T.*, **36**(4), 704-709.
- Zhang, Y.L. (2009), “Theoretical analysis and experimental research on behavior and crack control of negative moment zone in steel-concrete composite beams”. *Doctoral Dissertation*, Beijing Jiaotong University, 50, (*in Chinese*).

CC